Histochem Cell Biol (2013) 140:533–547
DOI 10.1007/s00418-013-1091-z

ORIGINAL PAPER

Cell-type-specific expression pattern of ceramide synthase 2 protein in mouse tissues

Christiane Kremser · Anna-Lena Klemm · Martina van Uelft · Silke Imgrund · Christina Ginkel · Dieter Hartmann · Klaus Willecke

Accepted: 20 March 2013 / Published online: 17 April 2013

Abstract Ceramide synthase 2 (CerS2) catalyzes the synthesis of dihydroceramides from dihydrosphingosine and very long fatty acyl (C22–C24)-CoAs. CerS2-deficient (gene trap) mice were reported to exhibit myelin and behavioral abnormalities, associated with the expression of CerS2 in oligodendrocytes and neurons based on expression of *lacZ* reporter cDNA instead of the *cers2* gene in these mice. In order to clarify the cell-type-specific expression of CerS2 protein, we have raised antibodies that specifically recognize the glycosylated and non-glycosylated CerS2 protein in wild-type but not in CerS2-deficient mouse tissues. In early postnatal, juvenile and adult mouse brain, the new antibodies detect CerS2 protein only in oligodendrocytes but not in neurons, suggesting that the gene trap vector in CerS2-deficient mice led to ectopic expression of the *lacZ* reporter gene in neurons. In liver, the CerS2 protein is expressed in hepatocytes but not in Ito cells or Kupffer cells. We conclude that the behavioral abnormalities observed in CerS2-deficient mice originate primarily in oligodendrocytes and not in neurons. The identification of specific cell types in which CerS2 protein is expressed is prerequisite to further mechanistic characterization of phenotypic abnormalities exhibited by CerS2-deficient mice. The amount of CerS2 protein detected in different tissues by immunoblot analyses does not strictly correspond to the activity of the CerS2 enzyme. Disproportional results are likely due to post-translational regulation of the CerS2 protein.

Keywords Brain · Ceramide synthase · Myelin · Oligodendrocytes · Sphingolipid

Introduction

Sphingolipids are major components of eukaryotic membranes and can function as signaling molecules in different pathways (Futerman and Hannun 2004). The molecular backbone of all complex sphingolipids are ceramides, which can also act as signaling molecules and are involved in differentiation, cell cycle control, apoptosis and neuronal development (Futerman and Hannun 2004; Ogretmen and Hannun 2004; Jana et al. 2009).

Ceramides consist of a long-chain sphingoid base, to which a fatty acid residue of different chain length is attached via an amide bond (Kolesnick et al. 2000). They can be synthesized via three different pathways: the de novo synthesis, in which dihydrosphingosine is *N*-acylated to dihydroceramide by ceramide synthases (CerS), the sphingomyelinase pathway, in which sphingomyelin of the plasma membrane is degraded to ceramide and phosphorylcholine by acid or neutral sphingomyelinase (Marchesini and Hannun 2004), and the salvage pathway, in which glycosphingolipids and sphingomyelin are degraded by several lysosomal enzymes (glycosidase, acid sphingomyelinase and acid ceramidase) to sphingosine (Kitatani et al. 2008). Sphingosine can then be acylated to ceramide by ceramide synthases.

Electronic supplementary material The online version of this article (doi:10.1007/s00418-013-1091-z) contains supplementary material, which is available to authorized users.

C. Kremser · A.-L. Klemm · M. van Uelft · S. Imgrund · C. Ginkel · K. Willecke (✉)
Molecular Genetics, Life and Medical Sciences (LIMES)-Institute, University of Bonn, Carl-Troll-Str. 31, 53115 Bonn, Germany
e-mail: k.willecke@uni-bonn.de

D. Hartmann
Division of Neuroanatomy, Department of Anatomy, University of Bonn, 53115 Bonn, Germany

Ceramide synthases are a family of highly conserved enzymes, members of which are expressed in all eukaryotes (Voelzmann and Bauer 2010). They were first identified in *Saccharomyces cerevisiae*, where the Lag1 and Lac1 proteins catalyze the de novo ceramide synthesis (Guillas et al. 2001; Schorling et al. 2001). In mammals, six CerS enzymes were identified (CerS1–6). CerS are transmembrane proteins of the endoplasmic reticulum (Riebeling et al. 2003; Laviad et al. 2008), which can be phosphorylated (Sridevi et al. 2009) and glycosylated (Mizutani et al. 2005; Ohno et al. 2010). Recently, it has been shown in transfected cells that the activity of tagged ceramide synthase proteins can be modulated via homo- and heteromeric dimerization (Laviad et al. 2012). Each CerS shows restricted substrate specificity towards the fatty acyl-CoA used for *N*-acylation. CerS2 and CerS4 prefer very long-chain fatty acyl-CoAs (C20:0–C24:0); CerS5 and CerS6 show a preference for shorter acyl-CoAs (C14:0–C16:0) (Mizutani et al. 2005). CerS3 exhibits reactivity towards a broad variety of acyl-CoAs including ultra-long fatty acid residues (C18:0–C36:0) (Mizutani et al. 2006; Jennemann et al. 2012), whereas CerS1 only catalyzes the synthesis of C18:0-dihydroceramide (Mizutani et al. 2005). In analogy to the acyl-CoA specificity, the *ceramide synthase* genes show different mRNA expression level in distinct tissues, which partially overlap. The *cers2* gene exhibits the highest transcript level of all *ceramide synthase* genes and is expressed in several tissues of the adult mouse, most notably in liver and kidney (Mizutani et al. 2005; Laviad et al. 2008). In addition, *cers2* mRNA was found by in situ hybridization in central and peripheral myelinating cells, in which its expression was upregulated during myelination (Becker et al. 2008).

Several years ago, we generated a CerS2-deficient (gene trap) mouse line (Imgrund et al. 2009). These mice carry a *lacZ* reporter gene controlled by the endogenous CerS2 promoter. Visualization of lacZ expression by staining for β-galactosidase in brain sections revealed expression of the *lacZ* gene in white and gray matter regions of cerebrum and cerebellum, suggesting expression of CerS2 protein in oligodendrocytes as well as in different types of neurons (Imgrund et al. 2009; Ben-David et al. 2011). CerS2-deficient mice exhibit various phenotypic abnormalities. In the central and peripheral nervous system of these mice, myelin degenerates during aging and detachment of myelin lamellae from axons is found (Imgrund et al. 2009; Ben-David et al. 2011). Furthermore, vacuolation in both gray and white matter regions was observed, accompanied by astrogliosis and microglia activation (Ben-David et al. 2011). In the liver, CerS2-deficient mice at 7–9 months develop multiple malignant hepatocarcinomata which appear to be formed by lipid- and glycogen-rich hepatocytes (Imgrund et al. 2009; Pewzner-Jung et al. 2010).

In order to study the cell-type-specific expression pattern of the CerS2 protein in more detail, we have raised CerS2-specific antibodies that recognize CerS2 protein only in wild-type cells, but did not exhibit any false-positive signal in CerS2-deficient tissues. These antibodies allow to correlate expression of the CerS2 protein with its potential function in different cell types in vivo and to study the regulatory consequences of dimer formation with other ceramide synthase proteins in distinct cell types. Thus, it will be possible to associate the different phenotypic abnormalities of CerS2-deficient mice with the cell-type-specific expression pattern of CerS2 protein.

Materials and methods

Animals

CerS2-deficient (gene trap) mice (abbreviated as CerS2 gt/gt) were generated as reported (Imgrund et al. 2009). The gene trap vector ROSAFARY had been inserted in intron 1 of the *cers2* gene and carries the coding region for the fusion protein βgeo, which codes for the enzyme β-galactosidase fused to a neomycin-resistance protein. The phosphoglycerate kinase promotor-driven hygromycin-resistance cassette was deleted by Flp-mediated recombination. $Cx47^{EGFP}$ mice carry an *egfp* reporter gene replacing the coding region of connexin (Cx) 47 after the first seven codons of Cx47 (Odermatt et al. 2003). Cx47 and therefore the eGFP reporter protein is expressed in oligodendrocytes and not in neurons.

Mice were kept under standard housing conditions with a 12-h/12-h dark/light cycle and with food and water ad libitum. Mice were raised in accordance with the instructions of local and state authorities regarding the use of animals for research purposes. All mice were backcrossed to at least 87.5 % C57BL/6 genetic background.

Cell culture

To obtain CerS2 +/+ and CerS2 gt/gt mouse embryonic fibroblast (MEFs), CerS2 +/gt mice were mated to each other, and mouse embryos from day 11.5 to 15.5 post-coitum were used. Pregnant mice were killed by cervical dislocation and the uteri were transferred to tissue culture plates (BD Bioscience, Germany) with sterile, pre-warmed (37 °C) Dulbecco's phosphate-buffered saline (DPBS, Life Technologies GmbH, Germany). The following steps were performed under a sterile hood. The uterus was removed and each embryo was transferred into a new culture plate. Yolks sacs, amnion, umbilical cord and extremities of each embryo were removed and carcasses were washed in fresh DPBS. Afterwards, carcasses were dissected and incubated

with trypsin solution (1 mM EDTA, 1 % chicken serum, 0.025 % Trypsin in DPBS) for 20 min at 37 °C to obtain single cells. The trypsin reaction was stopped by the addition of an appropriate amount of MEF medium (Glasgow medium containing 10 % fetal calf serum, 1 mM sodium pyruvate, 2 mM glutamine, 1× non-essential amino acids, 100 mg/ml streptomycin, 100 U/ml penicillin and 0.007 % β-mercaptoethanol). Single cells were separated from undigested tissue by a cell strainer (100 µm, BD Bioscience, Germany) and sedimented. Subsequently, cells were resuspended, transferred to gelatine-coated culture flasks and cultured at 37 °C in a humidified atmosphere containing 5 % CO_2.

Generation of rabbit polyclonal antibodies to a C-terminal peptide of CerS2

A 20-mer peptide of the C-terminal region (SRLLANGHPILNNNHPKND) of CerS2 was commercially synthesized in the laboratory of Prof. Egmond (Utrecht University, The Netherlands), coupled to keyhole limpet hemocyanin and injected into rabbits by Pineda Antikörper Service (Berlin, Germany). Sera were affinity purified via HiTrap NHS activated affinity columns (Amersham Bioscience, Germany), to which the mentioned peptide was bound. Antibodies were eluted with 0.2 M glycine (pH 2.5–3) and neutralized with 1 M Tris (pH 7.5–8). Then, they were dialysed over night against phosphate-buffered saline (PBS^-, 137 mM NaCl, 2,7 mM KCl, 8,1 mM Na_2HPO_4, 1,5 mM KH_2HPO_4, pH 7,4), concentrated in Microsep™ Centrifugal Devices (50 K) and stored in PBS^- with 1 % bovine serum albumin (BSA), 0.01 % sodium azide and 50 % glycerol at −20 °C.

Immunoblotting

Mice were killed by cervical dislocation. The different organs were prepared and quick-frozen in liquid nitrogen. Samples were homogenized in RIPA-buffer (10 mM phosphate buffer, pH 7.2, 0.1 % (w/v) SDS, 40 mM NaF, 2 mM EDTA, 1 % (v/v) TritonX-100, 0.1 % sodium deoxycholate) by a Precellys homogenisator (Peqlab Biotechnologie GmbH, Germany) and centrifuged for 5 min at 4 °C. The protein concentrations were determined using the Bicinchoninic acid kit for protein determination (Sigma, Germany). 50 µg of each protein lysate was denatured for 15 min at 72 °C in 2× urea buffer (40 mM Tris, 1 mM EDTA, 9 M urea, 5 % (w/v) SDS, 0.01 % (w/v) bromophenol blue, 5 % (v/v) 2-mercaptoethanol, pH 8) and separated via SDS-PAGE (12 %). Proteins were blotted onto nitrocellulose membranes (Hybond ECL, Amersham Bioscience), blocked with 5 % milk powder in Tris-buffered saline with 0.1 % Tween (TBST, 10 mM Tris, 150 mM NaCl, 0,1 % (v/v) Tween 20, pH 7,5) for 1 h at room temperature and incubated with CerS2 antibodies (1:1,000) diluted in blocking solution overnight at 4 °C. After washing in TBST, blots were incubated with horseradish peroxidase conjugated antibodies (1:10,000, Dianova) in TBST for 1 h at room temperature. Detection was carried out after three washing steps using the Super-Signal West Pico Chemiluminescent detection kit (Pierce) and exposure on X-ray films.

Immunoblots were standardized using a monoclonal mouse GAPDH antibody (Millipore, Germany) and horseradish peroxidase-conjugated secondary antibodies. Both were diluted 1:10.000 simultaneously in TBST and membranes were incubated for 45 min at room temperature.

Deglycosylation

Frozen samples of liver lobes from CerS2 +/+ and CerS2 gt/gt mice were extracted in homogenization buffer (20 mM Tris, 140 mM NaCl, 1 % TritonX-100, 10 % glycerol, 1 mM EGTA, 1.5 mM $MgCl_2$, protease inhibitors (complete EDTA-free Protease Inhibitor cocktail; Roche diagnostics), pH 7.4) and homogenized with a Precellys homogenisator (Peqlab Biotechnologie GmbH, Germany). For deglycosylation, 20 µg of protein lysates was denatured with 10× glycoprotein denaturing buffer for 10 min at 100 °C. Afterwards, samples were treated with 500 U of EndoH (New England Biolabs® Inc.) and 10× reaction buffer at 37 °C for 1 h. Subsequently, samples were mixed with 2× urea buffer, separated via SDS-PAGE and analyzed by immunoblotting.

Ceramide synthase assay

Preparation of tissue homogenates and ceramide synthase assays were performed as described (Kim et al. 2012) with minor modifications. Eight to ten-week-old mice were killed by cervical dislocation and tissue samples were homogenized in 20 mM HEPES–KOH (pH 7.4), 25 mM KCl, 250 mM sucrose, 2 mM $MgCl_2$, 2 mM EDTA and protease inhibitors with a Precellys homogenisator (Peqlab Biotechnologie GmbH, Germany) and centrifuged at 1,000*g* for 10 min. Aliquots of the crude tissue homogenate were frozen in liquid nitrogen and stored at −80 °C. Protein concentrations were determined using the Bicinchoninic acid kit (Sigma, Germany).

100 µg homogenate protein were diluted in homogenization buffer to a total volume of 50 µl and incubated with 10 µM NBD-sphinganine (omega(7-nitro-2-1,3-benzoxadiazole-4-yl)(2S,3R)-2-aminooctadecane-1,3-diol, Avanti Polar Lipids, USA) in 45 µl reaction buffer (20 mM HEPES–KOH pH 7.4, 25 mM KCl, 250 mM sucrose, 2 mM $MgCl_2$ and 0.34 mg/ml defated BSA (Sigma,

Germany)) for 2 min at 37 °C. The reactions were started with the addition of 50 µM C24:1-CoA (Avanti Polar Lipids, USA) and incubated for 20 min at 37 °C. Reactions were stopped and lipids were extracted by addition of 375 µl chloroform/methanol (1:2), chloroform (125 µl) and water (125 µl). After each step, samples were vortexed and centrifuged. The organic phase was dried under N_2-flow in a Reacti-Therm heating module (Thermo Fisher Scientific, Germany) and resuspended in 15 µl chloroform/methanol (1:1). Lipids were loaded on HPTLC silica gel 60 plates (Merck Millipore, Germany) and resolved in chloroform/methanol/water (8:1:0.1).

The fluorescence was detected by a LED lamp (10× 1 W 420 nm LEDs, Roithner Lasertechnik, Austria), equipped with a HEBO V01 (Hebo Spezialglas, Germany) excitation filter. Images were acquired with a Rolera MGI plus EMCCD camera (Decon Science Tec, Germany), equipped with a 494/20 and 572/28 bandpass emission filter wheel. All components were controlled by GelPro analyzer software (Media Cybernetics, USA). The fluorescent intensity was quantified using ImageJ (http://rsb.info.nih.gov/ij/index.html). For quantification of the fluorescence, the NBD-sphinanine standard was spotted onto the TLC plates in different amounts.

Immunofluorescence staining of cells

Mouse embryonic fibroblasts were grown on poly-L-lysine and gelatine-coated coverslips until they were confluent. The cells were fixed and stained as previously described (Jennemann et al. 2012) with antibodies to CerS2 (1:500), PDI (1:400, Acris, Germany) and GM130 (1:500, BD Bioscience, Germany). Nuclei were stained with Hoechst 33258 (1:5,000, Sigma, Germany). Images were taken with a two-photon laser scanning microscope (LSM 780, Zeiss, Germany).

Immunofluorescence staining of cryosections

Mice were killed by cervical dislocation; the different organs were dissected, embedded into TissueTek® (Sakura Finetek Germany GmbH, Germany) and frozen at −21 °C. Afterwards, organs were cut with a Leica cryostat CM3050 S in slices of 12 µm and collected on SuperFrost Ultra Plus slides (Menzel, Germany). Sections were air-dried for 15 min and fixed for 10 min in cold 100 % ethanol, methanol or acetone, depending on the tissue and the antibodies used. After fixation, slices were washed with Tris-buffer (50 mM Tris, 1.5 % (w/v) NaCl, 0.3 % (v/v) TritonX-100, pH 7.6) and blocked with 5 % normal goat serum (NGS) and 1 % BSA in Tris-buffer for 1 h at room temperature. Incubations with primary antibodies (CerS2 1:500, F4-80 1:300 (Abcam, USA), GFAP-Cy3 1:1,000 (Sigma, USA), NF200 1:1,000 (Abcam, USA)) were carried out overnight at 4 °C. Subsequently, slices were washed with Tris-buffer and incubated for 1 h with appropriate secondary antibodies coupled to Alexa Fluor® Dyes (1:1,000, Molecular Probes, Germany). Nuclei were stained with Hoechst 33258 (1:5,000, Sigma, Germany). Slices were washed with Tris-buffer and mounted with Fluorescence Mounting Medium (Dako Deutschland GmbH, Germany). The images were taken with the LSM 710 (Zeiss, Germany).

Immunofluorescence staining of vibratome sections

For immunostainings of the brain, mice were killed by an overdose of intraperitoneally injected anesthetic (5 mg/100 mg body weight of 10 % ketamine hydrochloride and 1 mg/100 mg body weight of 2 % xylazine hydrochloride) and transcardially perfused with 60 ml PBS^- followed by 60 ml phosphate-buffered formaldehyde solution (4 %, Roti-Histofix, Roth, Germany). The brains were quickly dissected and post-fixed over night in 4 % formaldehyde solution at 4 °C. Afterwards, brains were cut into free floating 25 µm sagittal sections with a vibratome (VT 1200 S, Leica, Germany), blocked with 5 % NGS, 1 % BSA, 0.5 % TritonX-100 in PBS^- for 1 h at room temperature and incubated with primary antibodies over night at room temperature (Calbindin 1:500 (Sigma, Germany), CerS2 1:1000, GFP 1:500 (Abcam, USA), NeuN 1:500 (Chemicon, Millipore GmbH, Germany), GFAP-Cy3 1:1,000 (Sigma, Germany)). Furthermore, sections were briefly washed with PBS^- and incubated with appropriate secondary antibodies coupled to Alexa Fluor® Dyes (1:1,000, Molecular Probes, Germany) for 2 h at room temperature. Nuclei were stained with Hoechst 33258 (1:5,000, Sigma, Germany). Afterwards, sections were washed with PBS^- and transferred into bidistilled water for at least 5 min. The sections were mounted on glass slides (Menzel, Germany), dried on a heating plate at 37 °C and mounted with Fluorescence Mounting Medium (Dako Deutschland GmbH, Germany).

Brains from mice of an age under P14 were embedded into liquid agar (2 % in PBS^-) to prevent tissue damage during sectioning. After solidification, brains were cut within agar blocks into sections of 75 µm and stained as described above.

β-Galactosidase and immunohistochemical staining of vibratome sections

For β-galactosidase staining, mice were killed by an overdose of intraperitoneally injected anesthetic and transcardially perfused with 60 ml PBS^- followed by 60 ml 2 % phosphate-buffered formaldehyde solution (Roti-Histofix, Roth, Germany), containing 0.2 % glutaraldehyde.

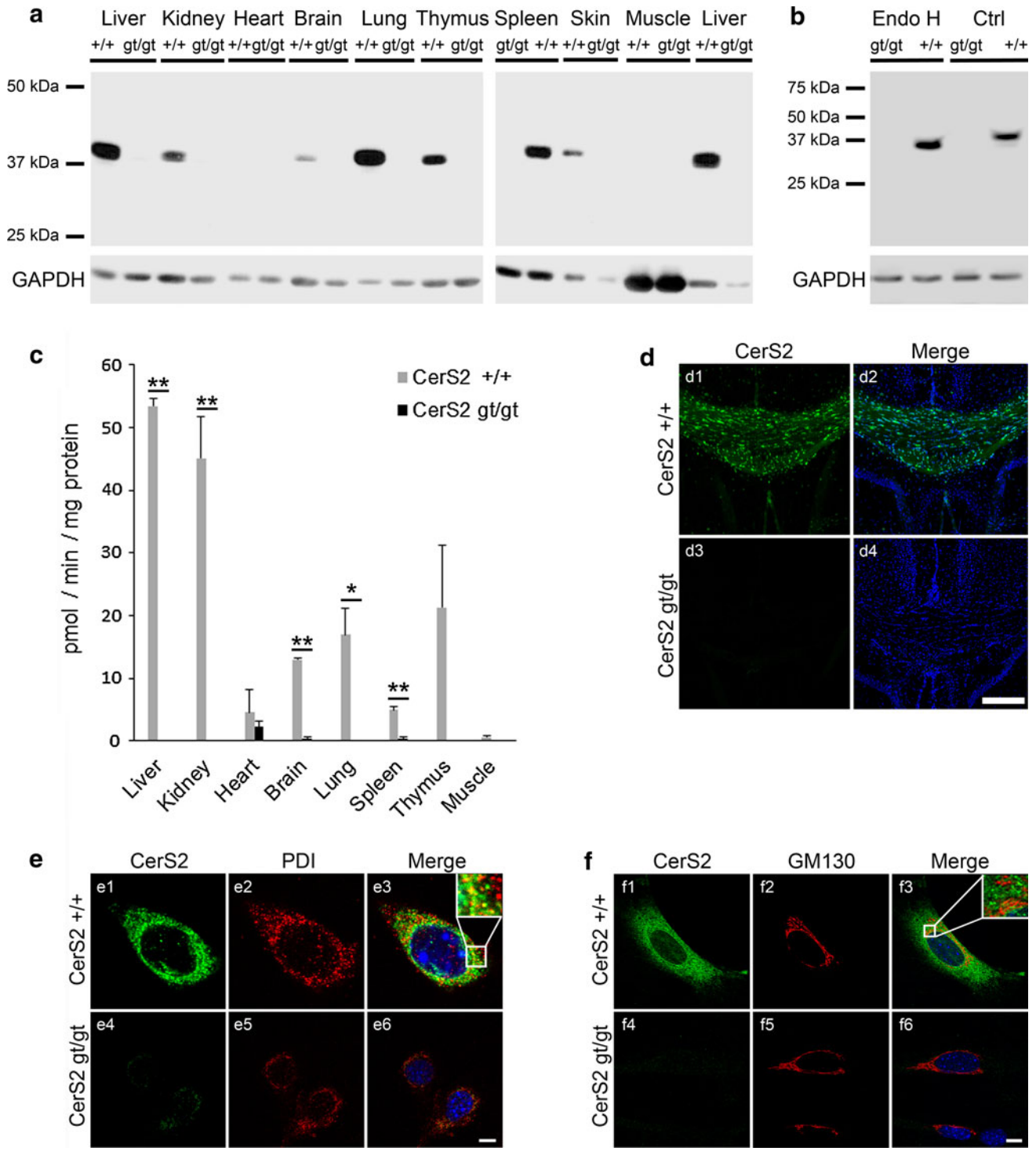

Fig. 1 Specificity of CerS2 antibodies and expression of CerS2 in different mouse tissues. **a** Immunoblot analyses using the newly generated antibodies against CerS2 show specific bands at 42 only for wild-type lysate. No bands were observed in CerS2 gt/gt (gene trap) lysates. **b** The CerS2 antibodies recognize glycosylated and deglycosylated CerS2 protein in liver lysates from CerS2 wild-type and gt/gt mice, treated with *EndoH* glycosylase or buffer alone and separated by electrophoresis. The immunoblot shows deglycosylated CerS2 protein at 37 kDa. **c** Ceramide synthase activity was tested in lysates from different organs of 8 to 10-week-old wild-type and *CerS2 gt/gt* mice using C24:1-CoA. No CerS-activity was measured in *CerS2 gt/gt* mice, except for heart and in very low amounts in liver, brain and spleen. Data shown are mean ± SEM ($n = 3$). *Statistically significant difference (*$p < 0.05$, **$p < 0.001$; *t* test) when compared with *CerS gt/gt* controls. **d** *CerS2* antibodies do not recognize protein in immunofluorescence analyses of *CerS2*-deficient brain sections including the corpus callosum. **e**, **f** Intracellular localization of CerS2 in primary mouse embryonic fibroblasts. CerS2 colocalizes partially with the ER-protein *PDI* (**e**), but not with GM130, a Golgi marker (**f**). Nuclei (*blue*) were stained with Hoechst 33258 (Sigma, Germany). *Scale bars* **d** 200 μm; **e**, **f** 10 μm

After removal, brains were post-fixed over night and cut into 25 µm free floating sections with a vibratome (VT 1200 S, Leica, Germany). β-Galactosidase staining was carried out according to Degen et al. 2004. The sections were stained over night, washed with LacZ washing solution and blocked in with 5 % NGS, 1 % BSA, and 0.5 % TritonX-100 in PBS^{-} for 1 h at room temperature. The incubation with the primary antibodies (CerS2 1:1,000) was done over night at room temperature followed by incubation with biotinylated secondary antibodies (1:400, Zymed, Life Technologies GmbH, Germany) at room temperature for 1 h. To enhance immunohistochemical staining, the Vectastain ABC Elite Kit (Vector Laboratories LTD. United Kingdom) was used in combination with the Vector NovaRED peroxidase substrate kit (Vector Laboratories LTD. United Kingdom) according to manufacturer's instructions. Stained sections were mounted on glass slides (Menzel, Germany), dried on a heating plate at 37 °C and mounted with Entellan (Merck Millipore Chemicals, Germany).

Results

Modification and intracellular localization of CerS2

In order to study the protein expression pattern of CerS2, we tested five commercial and custom-made antibodies. None of these distinguished between lysates of CerS2 wild type and CerS2-deficient mouse tissues in immunoblot analyses. Therefore, we generated new polyclonal rabbit CerS2 antibodies, raised against a C-terminal peptide of CerS2. The specificity of these antibodies was tested in immunoblot analyses and in immunofluorescence analyses of mouse tissues and cells (Fig. 1).

An immunoblot of different mouse tissues (Fig. 1a) yielded a band around 42 kDa. No bands were found in CerS2-deficient lysates. The highest expression of CerS2 protein was measured in liver and lung, followed by kidney, and spleen. In the thymus, the amount of CerS2 differed between all tested wild-type mice in a wide range, maybe due to the individual immunological status.

Fig. 2 Expression of CerS2 protein differs from β-galactosidase reporter protein expression in neurons of CerS2-deficient (gene trap) mice. **a1–3** CerS2 staining showed strong CerS2 expression in white matter tracts of the cerebrum (*corpus callosum*, *fimbria hippocampi*) and *cerebellum* of wild-type mice. Immunopositive cells were found next to pyramidal neurons (**a1** *arrows*) and some show extensions into the cingulum (**a1** *asterisk*). CerS2 staining was also found in the hippocampal alveus (**a2** *asterisk*). **b1–3** CerS2 and β-galactosidase staining of heterozygous CerS2-deficient mice. **c1–3** In double-stained heterozygous sections only few cells were positive for CerS2 and LacZ (*arrows*). **d1–3** β-galactosidase is highly expressed in the neurons of the cerebrum and cerebellum as well as in the white matter of CerS2-deficient mice. *Scale bars* **a**, **b**, **d** 200 µm; **c** 100 µm

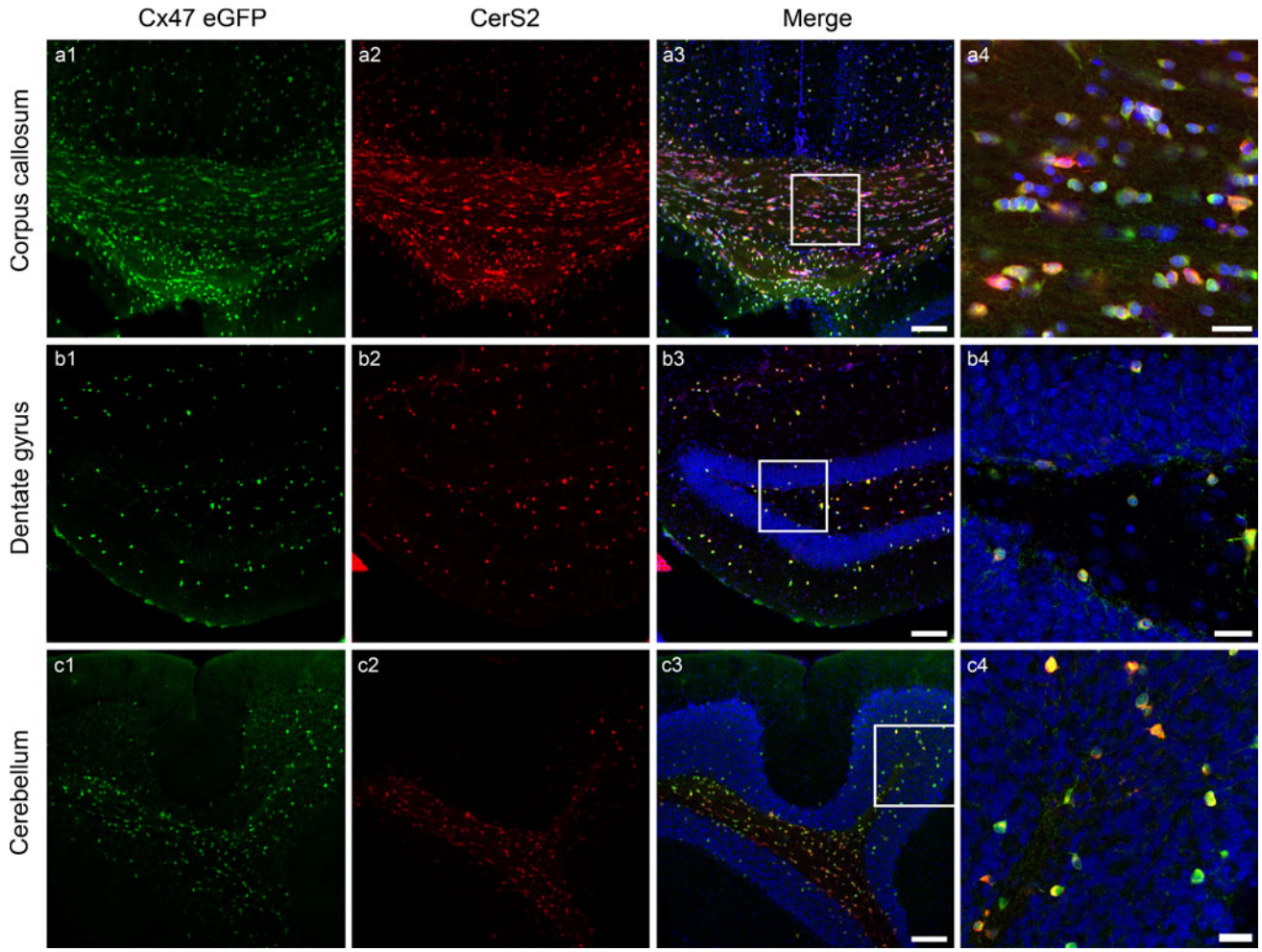

Fig. 3 CerS2 expression in mature oligodendrocytes. Adult heterozygous Cx47eGFP mice were used as reporter mice for mature oligodendrocytes (*green*) in the brain and stained for CerS2 (*red*). All CerS2-positive cells in the *corpus callosum* (**a**), *dentate gyrus* (**b**) and *cerebellum* (**c**) expressed Cx47eGFP, but not all eGFP-positive cells expressed CerS2. **a4**–**c4** Enlargement of *rectangles* in **a3**–**c3**. Nuclei (*blue*) were stained with Hoechst 33258. *Scale bars* **1**–**3** 100 μm; **4** 25 μm

Expression in brain and skin was considerably lower, whereas in heart and skeletal muscle, only a very weak band around 42 kDa was observed after longer exposure time (data not shown). An additional, apparently proteolytic band around 25 kDa was occasionally seen in wild-type lysates of liver, kidney, lung, spleen and thymus after longer exposure, but did not occur in every sample (data not shown). Previously, it was shown by in vitro experiments that a tagged CerS2 protein was *N*-glycosylated (Mizutani et al. 2005). Since we detected a double band for CerS2 in liver lysates (visible only after short exposure, data not shown) around the position of 42 kDa, we investigated the possibility of glycosylation in mouse liver. Therefore, we incubated lysates of both CerS2 wild-type and deficient liver with EndoH, a glycosidase which removes high mannose and some hybrid oligosaccharides of N-linked glycoproteins (Fig. 1b). In wild-type samples treated with EndoH, the upper band disappeared and only the lower band was visible at 37 kDa, whereas in untreated control, both bands were apparent. From these results, we conclude that most of the CerS2 protein is *N*-glycosylated in vivo.

In order to correlate the expression level of CerS2 protein with the enzyme activity, levels of ceramide synthase activity toward C24:1 acyl-CoA were tested in crude lysates of different organs of both 8 to 10-week-old wild-type and CerS2 gt/gt mice (Fig. 1c). The highest activity was measured in wild-type liver [53.5 ± 1.1 pmol/min/mg (mean ± SEM, $n = 3$)] and kidney (45.1 ± 6.6 pmol/min/mg), followed by thymus (21.3 ± 9.9 pmol/min/mg), lung (16.9 ± 4.3 pmol/min/mg), and brain (13 ± 0.2 pmol/min/mg). Lower activity levels were found in spleen (4.9 ± 0.7 pmol/min/mg), heart (4.5 ± 3.6 pmol/min/mg), and skeletal muscle (0.6 ± 0.2 pmol/min/mg). Some activity with C24:1-CoA in CerS2 gt/gt samples was found in heart (2.2 ± 1.0 pmol/min/mg) and in very low levels in brain (0.4 ± 0.2 pmol/min/mg) and spleen

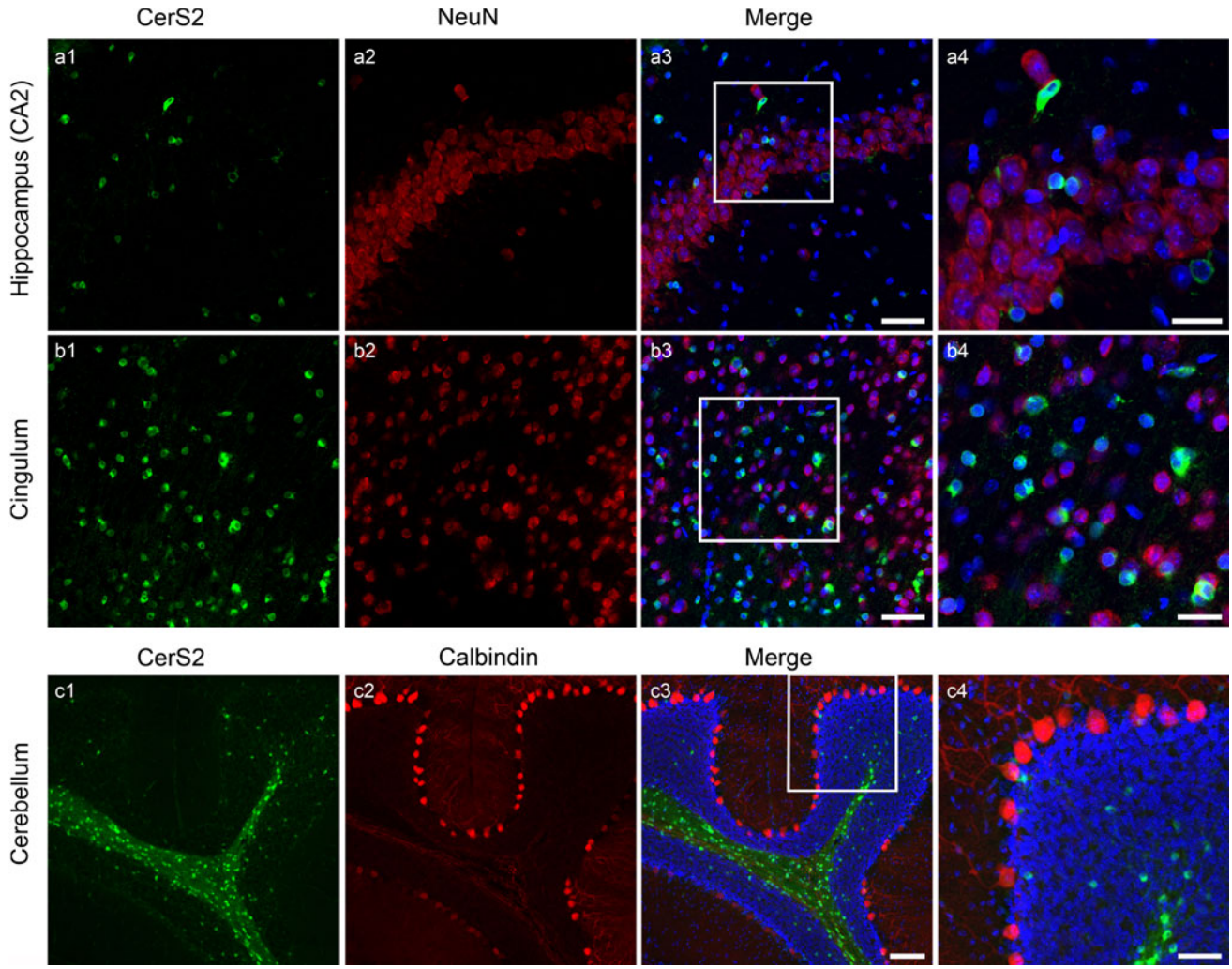

Fig. 4 CerS2 is not expressed in neurons. **a**, **b** CerS2 immunostaining (*green*) in hippocampus and *cingulum* of the adult mouse brain. CerS2 is not expressed in NeuN (*red*) positive neurons in both regions. **c** CerS2 immunostaining (*red*) in adult mouse *cerebellum*. CerS2 is not expressed in Purkinje cells (*green*, stained with *calbindin* antibodies). **a4**–**c4** Enlargement of *rectangles* in **a3**–**c3**. Nuclei (*blue*) were stained with Hoechst 33258. *Scale bars* **a1**–**3**, **b1**–**3** 50 μm; **a4**, **b4** 25 μm; **c1**–**3** 100 μm; **c4** 50 μm

(0.3 ± 0.3 pmol/min/mg). Activity was undetectable in CerS2 gt/gt lysates of liver, kidney, lung, thymus, and skeletal muscle. In crude lysates of the skin, we were not able to measure the CerS activity due to high background signals. In immunofluorescence analyses of mouse brain sections, the CerS2 antibodies yielded strong signals in wild-type sections (Fig. 1d1-2), whereas no protein was recognized for example in the corpus callosum of CerS2-deficient mice (Fig. 1d3-4).

In order to demonstrate the subcellular localization of CerS2 in vivo, we used primary mouse embryonic fibroblasts from CerS2 wild-type and CerS2-deficient mice for co-immunofluorescence analyses with marker proteins. The mouse CerS2 protein colocalizes partially with the protein disulfide isomerase (PDI, Fig. 1e), which is localized in the rough endoplasmic reticulum. It is not localized in the Golgi apparatus which is stained with a GM130 antibody (Fig. 1f) underlining again the specificity of the new CerS2 antibodies.

CerS2 expression in the central and peripheral nervous system

In previously published studies using the CerS2 gene trap mouse line, the *lacZ* reporter gene was used for indirect analyses of CerS2 expression. The *lacZ* reporter is part of the integrated gene trap and therefore expressed under the control of the endogenous *cers2* promoter. β-Galactosidase stainings showed distinct expression in both neurons and oligodendrocytes. To check these findings, combined β-galactosidase and immunohistochemical CerS2 stainings of standardized frontal sections of the parietal isocortex and associated hippocampal formation as well as sagittal sections of the cerebellar vermis were carried out (Fig. 2).

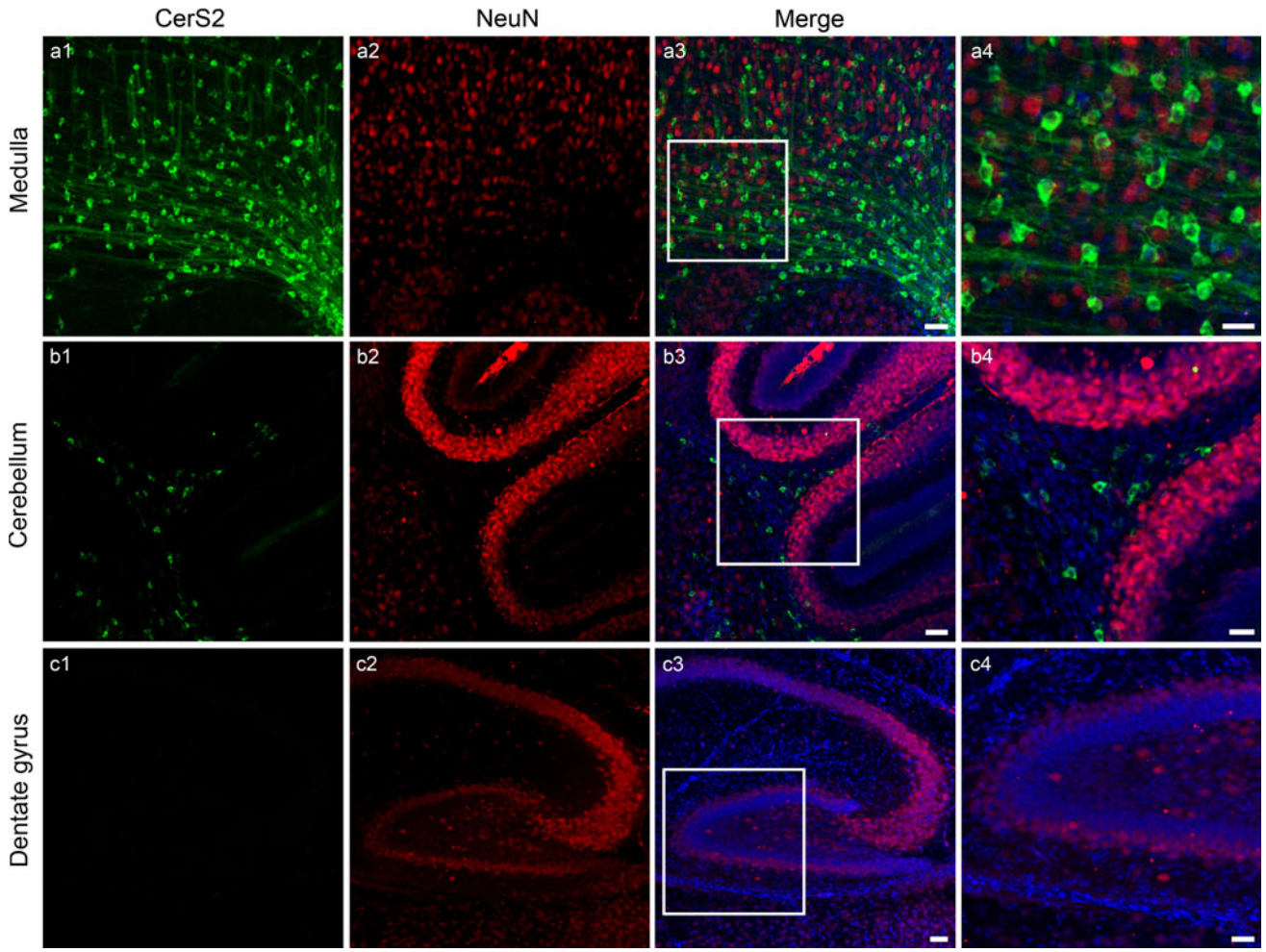

Fig. 5 CerS2 expression during brain development on P7. **a** Immunofluorescence stainings on brain sections showed strong expression of CerS2 (*green*) in mature oligodendrocytes of the *medulla*. **b** Scattered CerS2-positive cells were detected in the white matter of the *cerebellum*. **c** CerS2 is not expressed in the *dentate gyrus* and other cerebral regions. (**a4–d4**) Enlargement of *rectangles* indicated in **a3–c3**. Nuclei (*blue*) were stained with Hoechst 33258. *Scale bars* **1–3** 50 μm; **4** 25 μm

In wild-type mice and mice heterozygous for the CerS2-deficient allele (Fig. 2a, b), CerS2 staining by immunohistochemistry yielded signals mainly restricted to white matter tracts of cerebrum and cerebellum, like corpus callosum, fimbria hippocampi, and the white matter of the cerebellum.

In the isocortex, scattered immunopositive cells were observed especially within the deep laminae (V and often VI) next to pyramidal neurons (arrows), thus mainly representing glia cells. Note also the extension of immunopositive cells into the cingulum (asterisk), a cortical association fiber tract (Fig. 2a1), which also correspond to glial rather than to neuronal cells.

Within the hippocampal formation and lateral ventricles (Fig. 2a2), both ependymal cells and plexus epithelium stained CerS2 positive. Lateral to the CA2/CA3, the hippocampal alveus (asterisk) collecting myelinated pyramidal cell axons likewise stained positive before entering the fimbria. Both within the stratum pyramidale and stratum oriens, but rarely in the stratum moleculare, immunopositive cells were seen with smaller somata than pyramidal cells, rendering them mainly scattered glia cells.

In the cerebellum (Fig. 2a3), CerS2-immunopositive cells outside of the white matter are mainly found within the internal granular layer and rarely wedged inbetween Purkinje cells, whereby the latter would correspond to a subgroup of Bergmann glia.

In contrast to immunohistochemical CerS2 staining, LacZ stainings in gene trap mice (Fig. 2d) indicate a clear and widespread neuronal expression of different staining intensities. The highest expression of the reporter protein was seen in the CA1 region of the hippocampus, followed by the dentate gyrus and the neocortical layers (Imgrund et al. 2009).

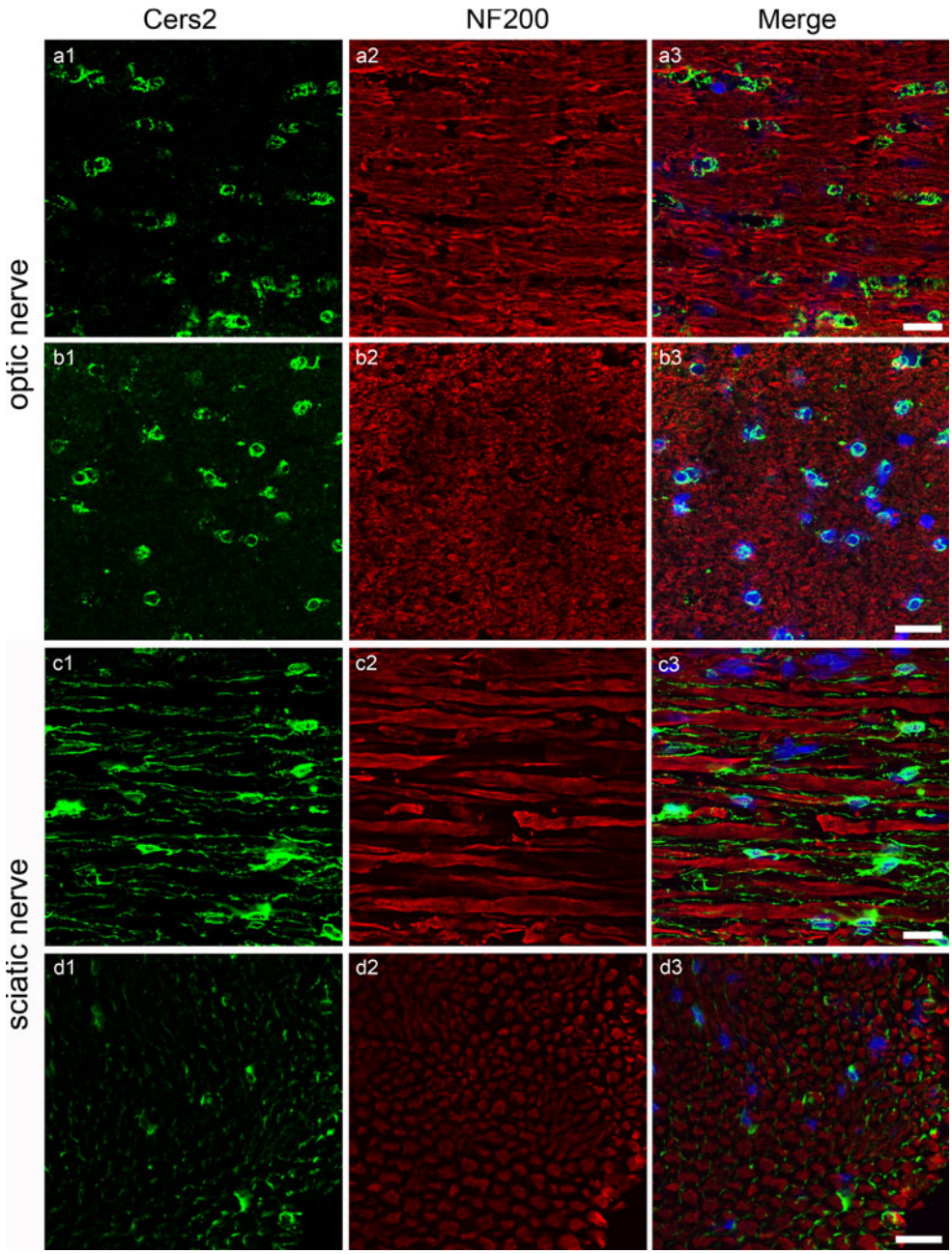

Fig. 6 CerS2 expression in the nerve fibers. Immunostainings for *CerS2* (*green*) and the neurofilament marker protein *NF200* (*red*) on longitudinal section (**a**) and cross section (**b**) of the myelinated part of the *optic nerve* show distinct expression in the somata of oligodendrocytes. In the *sciatic nerve* CerS2 is expressed in the somata of Schwann cells and along the myelin as shown in longitudinal (**c**) and cross sections (**d**). Nuclei (*blue*) were stained with Hoechst 33258. *Scale bars* 25 μm

In double-stained heterozygous brain sections (Fig. 2b), the LacZ staining did not overlap with the protein expression of CerS2 in most cells. Only few LacZ-positive cells were stained for CerS2 in the cingulum, oriens layer, fimbria, and thalamus (Fig. 2c arrows, enlarged from b), but there were no cells positive for CerS2 and LacZ in the hippocampus, dentate gyrus, and neocortex layers. In contrast, the principal neurons forming the hippocampal layers, i.e. pyramidal neurons of CA1–CA4 as well as the granule cells of the dentate gyrus did not exhibit CerS2 immunoreactivity. To investigate whether CerS2 is expressed in oligodendrocytes, in neurons or in both cell types, we performed co-immunofluorescence analyses with cell-type-specific marker. For the identification of oligodendrocytes in wild-type mouse brain, we used adult $Cx47^{eGFP(+/-)}$ mice, in which Connexin (Cx) 47 is replaced by an enhanced green fluorescent reporter protein (eGFP) under control of the Cx47 promoter. Cx47 is expressed in oligodendrocytes of highly myelinated CNS tissues as well as in few S100β-positive astrocytes, but not in neurons (Odermatt et al. 2003). Thus, it can be used as marker for oligodendrocytes in mice. The double-staining for Cx47 eGFP and CerS2 confirmed the oligodendrocyte-specific expression of CerS2 protein in adult mouse brain (Fig. 3).

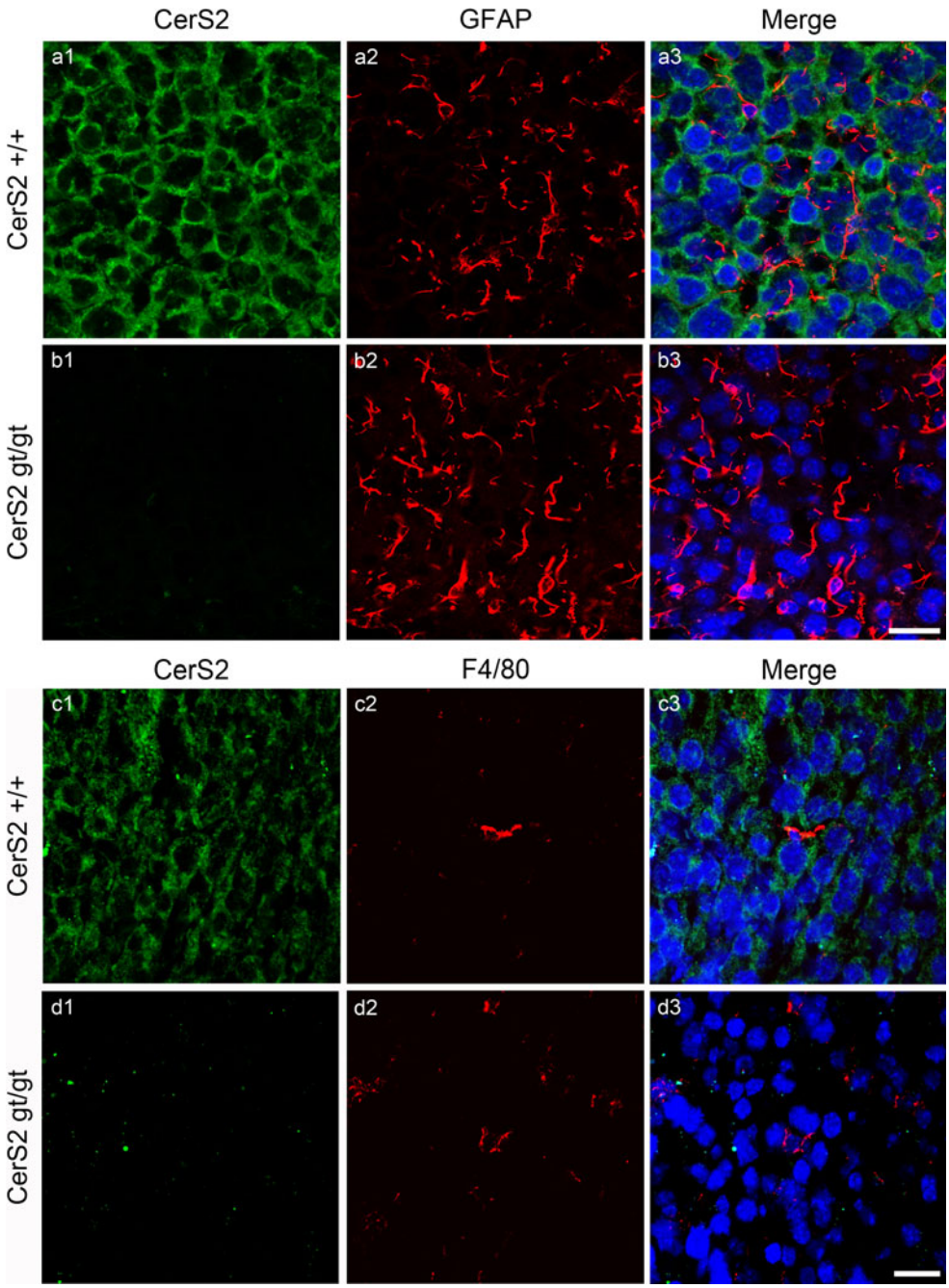

Fig. 7 CerS2 expression in the liver. **a1–d3** Immunostaining indicate that CerS2 protein (*green*) is expressed in hepatocytes, but not in Ito cells (**a**–**b**, *red*, stained for GFAP) or Kupffer cells (**c**–**d**, *red*, stained for F4-80) of wild-type mice. Nuclei (*blue*) were stained with Hoechst 33258. *Scale bars* 25 μm

All CerS2 expressing cells were positive for Cx47 eGFP in the corpus callosum (Fig. 3a), in the dentate gyrus (Fig. 3b) and the cerebellum, where only few cells were stained. Here, most of the double-stained cells were localized in the white matter and few were found in the internal granule cell layer and the ganglionar cell layer (Fig. 3c). CerS2 appears to be localized in the somata of adult oligodendrocytes.

Double-staining with antibodies to CerS2 and the neuronal nuclear antigen NeuN showed no overlapping expression. In sections of the hippocampal CA2 region (Fig. 4a), the CerS2-positive cells are located next to the neurons, but CerS2 is not expressed in neurons. The same was seen in the cingulum, a prominent myelinated intracortical fiber tract. CerS2-positive cells were visible in direct neighborhood to neurons but the signals did not overlap (Fig. 4b). Based on immunohistochemical staining against CerS2 in cerebellum, where few CerS2-positive cells were found in the ganglionar layer, we stained cerebellar sections for calbindin, a calcium-binding protein, which is specific for Purkinje cells in the cerebellum. As shown in Fig. 4c, CerS2 is not expressed in Purkinje cells,

but in cells close to them. Most likely, CerS2 protein resides in the somata of Bergmann glia cells.

Furthermore, we stained brain sections for GFAP-positive astrocytes to investigate whether or not CerS2 is expressed in astrocytes. As shown in the Supplementary Fig. S1, CerS2 is not localized in astrocytes except for Bergmann glia in adult wild-type mice, but CerS2-deficient mice showed very strong astrogliosis, especially in white matter regions like cingulum, cerebellar white matter (Supplementary Fig. S1 b, d), and in corpus callosum at an age of only 8 weeks. In gray matter regions like hippocampus and neocortex, no difference between CerS2 wild-type and deficient mice was observed.

We analyzed the cell-type-specific expression of CerS2 during postnatal brain development. On P21, CerS2 was found in exactly the same expression pattern as in adult mouse brain (data not shown). In contrast, on P7, the expression of CerS2 is restricted to the brainstem, where strong CerS2 signals were found in both the soma and processes of oligodendrocytes in medulla (Fig. 5a), pons, white matter of cerebellum (Fig. 5b) and within the midbrain, which confirms the expression in myelinating oligodendrocytes. CerS2 protein was not found within the dentate gyrus, and other cerebral regions (Fig. 5c). On P2, CerS2 was found only in brainstem, medulla and pons, but not in the white matter of the cerebellum. The same result was observed with newborn mice. Here, CerS2 expression was restricted to the brainstem and the medulla (data not shown). Since the expression of CerS2 protein appears to follow the migration and differentiation of oligodendrocyte precursor cells of the third wave, we conclude that CerS2 is highly expressed in mature oligodendrocytes during myelination (Richardson et al. 2006; Bradl and Lassmann 2010).

In order to investigate CerS2 protein expression in central tracts and peripheral nerves, we co-stained longitudinal sections and cross sections of the optic nerve and the sciatic nerve against CerS2 and neurofilament H (NF200), a neuron-specific protein. In the optic nerve, CerS2 was found in the somata of oligodendrocytes (Fig. 6a, b), but not along myelinated axons or their myelin sheath outside of oligodendrocyte somata. In contrast to this, stainings of the sciatic nerve showed strong signals in somata of Schwann cells and along the myelin sheath in longitudinal and cross sections (Fig. 6c, d).

CerS2 expression in mouse liver

We wanted to test the specificity of the new CerS2 antibodies also in liver, since the *cers2* gene is highly expressed in this organ. Double immunofluorescence stainings with different cell type markers were carried out. As illustrated in Fig. 7a–d, CerS2 protein is expressed in hepatocytes of mouse liver, which were identified by their morphology. Double-stainings revealed that CerS2 protein was not present in Ito cells, which were stained with a GFAP antibody (Fig. 7a, b), or in Kupffer cells, which were stained with a F4-80 antibody (Fig. 7c, d). Both cell types are relatively small and were localized next to the CerS2-positive hepatocytes. The CerS2 antibodies do not detect any specific signals in sections of CerS2-deficient mice (Fig. 7b, d).

Discussion

The new antibodies characterized in this study are to our knowledge the first which recognize CerS2 protein in specific cell types, without false-positive signals in knockout material. We have developed these antibodies to solve the discrepancy that *cers2* mRNA has been found by in situ hybridization at high level in mouse oligodendrocytes (Becker et al. 2008), whereas the expression of the *lacZ* reporter gene instead of CerS2 in transgenic mice reported by two groups (Imgrund et al. 2009; Pewzner-Jung et al. 2010; Ben-David et al. 2011) indicated that the *cers2* gene is expressed in oligodendrocytes and neurons of mouse brain. The new antibodies characterized in this study clearly show that postnatally the CerS2 protein is expressed in myelin-forming cells but not in neurons.

As also shown in this study, the CerS2 protein is highly expressed in liver and lung, followed by spleen, kidney, and brain. Lower amounts were found in skin, whereas in heart and skeletal muscle, the expression of CerS2 protein was very low. In the thymus, the protein level of CerS2 as well as the enzymatic activity toward C24:1-CoA differed between all tested wild-type mice in a wide range, probably due to the individual immunological status. To correlate the protein level of CerS2 with the enzymatic activity of CerS2, ceramide synthase assays were done with C24:1-CoA and NBD-sphinganine as substrate. As shown, the activities against C24:1-CoA are inconsistent with the protein levels in some organs, especially the lung. The highest enzyme activity was measured in liver and kidney, followed by thymus, lung, and brain. Only low activity was detected in spleen, heart, and skeletal muscle. These results differ from previous reports where the expression of *cers2* mRNA (Riebeling et al. 2003; Mizutani et al. 2005; Laviad et al. 2008) and the *N*-acyl chain length of different sphingolipids (Laviad et al. 2008; Ben-David et al. 2011) were analyzed. Especially in the brain, the *cers2* mRNA expression was relatively low in contrast to the higher level of CerS2 protein, enzymatic activity and C22- and C24-sphingolipids, which hint that CerS2 expression can be post-translationally modulated. In contrast, in lung, *cers2* mRNA level is low, according to the enzyme activity,

whereas CerS2 protein is expressed at a high level. Recently, it was reported by Laviad et al. (2012) that CerS2 can form homo and heterodimers with other CerS proteins in transfected overexpressing cells, which can lead to enhanced enzymatic activity.

The new CerS2 antibodies recognize both the glycosylated and also the non-glycosylated form of CerS2 protein after treatment with EndoH glycosylase in protein extracts. In all mouse tissues investigated in this study, the glycosylated form of CerS2 protein is prevalent. Until now, little is known about the function of this modification. *N*-glycosylation of CerS does not alter the enzyme activity (Mizutani et al. 2005), but may play a role in the regulation of the interaction between CerS2 and other proteins like Elovl1 (Ohno et al. 2010). In agreement with prior studies on transfected cells which express a tagged CerS2 protein (Laviad et al. 2008, 2012), we show that endogenous CerS2 protein is located in the endoplasmic reticulum. Since the CerS2 gene trap mice carry a *lacZ* reporter gene under the control of the *cers2* promoter, prior studies used β-galactosidase activity for indirect analyses of the CerS2 expression. The β-galactosidase stainings showed a widespread neuronal expression in different brain regions as well as strong expression in white matter regions and it differed between gray and white matter. In the gray matter, β-galactosidase staining appeared dotted, whereas in the white matter staining appeared uniform and not punctated (Imgrund et al. 2009; Ben-David et al. 2011). Previous in situ hybridizations of *cers2* mRNA had indicated that *cers2* mRNA expression is limited to oligodendrocytes and Schwann cells (Becker et al. 2008). The double-staining for CerS2 and LacZ as well as double immunofluorescence analyses with different markers for oligodendrocytes, neurons and astrocytes (Supplementary Fig. S1) confirmed the cell-type-specific expression of CerS2 protein in oligodendrocytes and Schwann cells, in agreement with the study of Becker et al. (2008) using in situ hybridization of *cers2* mRNA.

Thus, the deposition of a membranous storage material in astrocytes of CerS2-deficient mice described by Ben-David et al. (2011) cannot be due to missing expression of CerS2 in astrocytes but is likely caused by loss of CerS2 in oligodendrocytes. In confirmation of Ben-David et al. (2011), we also noticed strong astrogliosis in white matter of CerS2-deficient brain (cf. Supplementary Fig. S1). Again this cannot be an astrocyte autonomous effect but is possibly due to the described abnormalities in myelination of CerS2-deficient oligodendrocytes.

These observations led us to conclude that the *lacZ* reporter gene expression did not correlate with the expression of CerS2 protein after birth. Since the gene trap is integrated into intron1 of the *cers2* gene (Imgrund et al. 2009), a fusion protein of cers2 exon 1 and the β-galactosidase/neomycin reporter cassette of the gene trap vector is expressed, whereas the second transcript derived from the hygromycin resistance gene fused to *cers2* exon 2–11 sequence is not transcribed (Imgrund et al. 2009). The *lacZ* transcript does not contain the 3′UTR of the *cers2* transcript. Thus, it is possible that missing microRNA binding sites in the 3′UTR of the mutated *cers2* gene may affect the expression of the reporter protein in the brain. MicroRNAs can regulate neural development. Several brain-specific microRNAs are time-dependently expressed in specific cell populations and can regulate cellular differentiation and development (Enciu et al. 2012). Two microRNA prediction programs, TargetScan and miRBase, predicted several putative miRNA binding sites for different miRNAs within the *cers2* 3′UTR. For the neuronal miRNA miR-124, it was previously shown by microarray analyses after miR-124 transfection in different cell lines that miR-124 is able to downregulate the mRNA level of *cerS2* in vitro (Lim et al. 2005; Yu et al. 2008).

We detected strong expression of CerS2 protein in processes of oligodendrocytes during postnatal brain development (p0–p21), but not in adult mice, which indicates the high expression level of CerS2 during active myelination. This is consistent with the postnatally increasing amount of C22–C24 hexosylceramides, which are major components of myelin and consist mostly of galactosylceramides. The levels of galactosylceramides and sulfatides increase strongly during differentiation of oligodendrocytes as well as parallel to the proceeding myelination and became predominant in adult mouse brain, whereas glucosylceramides were predominantly expressed during embryonic development (Ngamukote et al. 2007; Yu et al. 2009). In CerS2-deficient brain, the amount of galactosylceramide is strongly reduced as reported by Imgrund et al. (2009) and Ben-David et al. (2011).

Interestingly, in the optic nerve, which is a part of the central nervous system, we found that the CerS2 protein is highly expressed in somata of mature oligodendrocytes, whereas in Schwann cells of the sciatic nerve, CerS2 was found in somata and myelin sheaths (Fig. 6). This may be due to differences in the structure of peripheral and central myelin sheaths. In myelin sheaths of oligodendrocytes, the outer cytoplasm forms a short, tongue-like structure, which covered only a short region of the myelinated axon, whereas Schwann cell myelin sheaths contain a continuous layer of cytoplasm, which surrounds the myelin spiral in addition to the internal cytoplasm of the first myelin turn (Peters 1960). It was previously shown that the smooth endoplasmic reticulum of Schwann cells reaches from the perinuclear to the paranodal cytoplasm (Gould and Sinatra 1981; Trapp et al. 1995) and certain lipids are synthesized in the smooth endoplasmic reticulum of the myelin internodes (Gould and Sinatra 1981; Gould et al. 1987). Since

we found CerS2 only partially colocalized with the rough endoplasmic reticulum markers of wild-type mouse embryonic fibroblasts, it is possible that it is localized in the smooth endoplasmic reticulum. Due to the fact that only peripheral myelin sheath contains cytoplasm in the outer myelin layer, CerS2 in the central myelin sheaths of mature oligodendrocytes may not be stained.

From our results regarding the cell-type-specific expression of CerS2 in oligodendrocytes and Schwann cells, we conclude that the strong behavioral and myelin abnormalities in CerS2-deficient mice (Imgrund et al. 2009; Ben-David et al. 2011) are likely due to the loss of expression in oligodendrocytes and Schwann cells but not primarily in neurons.

The liver is the organ with the highest *cers2* mRNA expression level (Mizutani et al. 2005; Laviad et al. 2008). In contrast, LacZ staining in the liver of CerS2 gt/gt mice was relatively weak (Imgrund et al. 2009). Staining of CerS2 wild-type liver sections with CerS2 antibodies revealed specific CerS2 staining in hepatocytes, but not in Ito and Kupffer cells. This is consistent with an increased extent of apoptosis and proliferation of hepatocytes in young CerS2-deficient mice as well as during development of hepatocellular carcinomas in CerS2-deficient mice (Imgrund et al. 2009; Pewzner-Jung et al. 2010).

In summary, our new CerS2 antibodies specifically recognize the CerS2 protein in wild-type cells but do not detect this protein in CerS2-deficient cells. Our analyses indicate specific expression of CerS2 protein in oligodendrocytes and Schwann cells as well as in hepatocytes. These antibodies should be useful to further correlate phenotypic abnormalities in CerS2-deficient mice with the loss of CerS2 protein in myelinating cells and in hepatocytes as well as to analyze post-translational modifications and the regulatory consequences of dimer formation of CerS2 with other ceramide synthase proteins in different organs.

Acknowledgments We thank D. May for providing $Cx47^{EGFP}$ mice, Dr. S. Sonntag for his support during this project and C. Siegmund for excellent technical assistance. Furthermore we thank Prof. M. Egmond (Utrecht) for providing the immunogenic CerS2 peptide. This study was supported by a grant of the German Research Foundation (through SFB 645, B2) to K. W.

References

Becker I, Wang-Eckhardt L, Yaghootfam A, Gieselmann V, Eckhardt M (2008) Differential expression of (dihydro)ceramide synthases in mouse brain: oligodendrocyte-specific expression of CerS2/Lass2. Histochem Cell Biol 129:233–241

Ben-David O, Pewzner-Jung Y, Brenner O, Laviad EL, Kogot-Levin A, Weissberg I, Biton IE, Pienik R, Wang E, Kelly S, Alroy J, Raas-Rothschild A, Friedman A, Brugger B, Merrill AH, Futerman AH (2011) Encephalopathy caused by ablation of very long acyl chain ceramide synthesis may be largely due to reduced galactosylceramide levels. J Biol Chem 286:30022–30033

Bradl M, Lassmann H (2010) Oligodendrocytes: biology and pathology. Acta Neuropathol 119:37–53

Degen J, Meier C, Van Der Giessen RS, Söhl G, Petrasch-Parwez E, Urschel S, Dermietzel R, Schilling K, De Zeeuw CI, Willecke K (2004) Expression pattern of lacZ reporter gene representing connexin36 in transgenic mice. J Comp Neurol 473:511–525

Enciu A-M, Popescu BO, Gheorghisan-Galateanu A (2012) MicroRNAs in brain development and degeneration. Mol Biol Rep 39:2243–2252

Futerman AH, Hannun Ya (2004) The complex life of simple sphingolipids. EMBO Rep 5:777–782

Gould RM, Sinatra RS (1981) Internodal distribution of phosphatidylcholine biosynthetic activity in teased peripheral nerve fibres: an autoradiographic study. J Neurocytol 10:161–167

Gould RM, Holshek J, Silverman W, Spivack WD (1987) Localization of phospholipid synthesis to Schwann cells and axons. J Neurochem 48:1121–1131

Guillas I, Kirchman PA, Chuard R, Pfefferli M, Jiang JC, Jazwinski SM, Conzelmann A (2001) C26-CoA-dependent ceramide synthesis of *Saccharomyces cerevisiae* is operated by Lag1p and Lac1p. EMBO J 20:2655–2665

Imgrund S, Hartmann D, Farwanah H, Eckhardt M, Sandhoff R, Degen J, Gieselmann V, Sandhoff K, Willecke K (2009) Adult ceramide synthase 2 (CERS2)-deficient mice exhibit myelin sheath defects, cerebellar degeneration, and hepatocarcinomas. J Biol Chem 284:33549–33560

Jana A, Hogan EL, Pahan K (2009) Ceramide and neurodegeneration : susceptibility of neurons and oligodendrocytes to cell damage and death. J Neurol Sci 278:5–15

Jennemann R, Rabionet M, Gorgas K, Epstein S, Dalpke A, Rothermel U, Bayerle A, Van der Hoeven F, Imgrund S, Kirsch J, Nickel W, Willecke K, Riezman H, Gröne H-J, Sandhoff R (2012) Loss of ceramide synthase 3 causes lethal skin barrier disruption. Hum Mol Genet 21:586–608

Kim HJ, Qiao Q, Toop HD, Morris JC, Don AS (2012) A fluorescent assay for ceramide synthase activity. J Lipid Res 53:1701–1707

Kitatani K, Idkowiak-Baldys J, Hannun Ya (2008) The sphingolipid salvage pathway in ceramide metabolism and signaling. Cell Signal 20:1010–1018

Kolesnick RN, Goñi FM, Alonso A (2000) Compartmentalization of ceramide signaling: physical foundations and biological effects. J Cell Physiol 184:285–300

Laviad EL, Albee L, Pankova-Kholmyansky I, Epstein S, Park H, Merrill AH, Futerman AH (2008) Characterization of ceramide synthase 2: tissue distribution, substrate specificity, and inhibition by sphingosine 1-phosphate. J biol chem 283:5677–5684

Laviad EL, Kelly S, Merrill AH, Futerman AH (2012) Modulation of ceramide synthase activity via dimerization. J biol chem 287:21025–21033

Lim LP, Lau NC, Garrett-Engele P, Grimson A, Schelter JM, Castle J, Bartel DP, Linsley PS, Johnson JM (2005) Microarray analysis shows that some microRNAs downregulate large numbers of target mRNAs. Nature 433:769–773

Marchesini N, Hannun YA (2004) Acid and neutral sphingomyelinases: roles and mechanisms of regulation. Biochem Cell Biol 82:27–44

Mizutani Y, Kihara A, Igarashi Y (2005) Mammalian Lass6 and its related family members regulate synthesis of specific ceramides. Biochem J 390:263–271

Mizutani Y, Kihara A, Igarashi Y (2006) LASS3 (longevity assurance homologue 3) is a mainly testis-specific (dihydro)ceramide

synthase with relatively broad substrate specificity. Biochem J 398:531–538

Ngamukote S, Yanagisawa M, Ariga T, Ando S, Yu RK (2007) Developmental changes of glycosphingolipids and expression of glycogenes in mouse brains. J Neurochem 103:2327–2341

Odermatt B, Wellershaus K, Wallraff A, Seifert G, Degen J, Euwens C, Fuss B, Büssow H, Schilling K, Steinhäuser C, Willecke K (2003) Connexin 47 (Cx47)-deficient mice with enhanced green fluorescent protein reporter gene reveal predominant oligodendrocytic expression of Cx47 and display vacuolized myelin in the CNS. J Neurosci 23:4549–4559

Ogretmen B, Hannun Ya (2004) Biologically active sphingolipids in cancer pathogenesis and treatment. Nat Rev Cancer 4:604–616

Ohno Y, Suto S, Yamanaka M, Mizutani Y, Mitsutake S, Igarashi Y, Sassa T, Kihara A (2010) ELOVL1 production of C24 acyl-CoAs is linked to C24 sphingolipid synthesis. Proc Nat Acad Sci USA 107:18439–18444

Peters A (1960) The formation and structure of myelin sheath in the central nervous system. J Biophys Biochem Cytol 8:431–446

Pewzner-Jung Y, Brenner O, Braun S, Laviad EL, Ben-Dor S, Feldmesser E, Horn-Saban S, Amann-Zalcenstein D, Raanan C, Berkutzki T, Erez-Roman R, Ben-David O, Levy M, Holzman D, Park H, Nyska A, Merrill AH, Futerman AH (2010) A critical role for ceramide synthase 2 in liver homeostasis: II. insights into molecular changes leading to hepatopathy. J Biol Chem 285:10911–10923

Richardson WD, Kessaris N, Pringle N (2006) Oligodendrocyte wars. Nat Rev Neurosci 7:11–18

Riebeling C, Allegood JC, Wang E, Merrill AH, Futerman AH (2003) Two mammalian longevity assurance gene (LAG1) family members, trh1 and trh4, regulate dihydroceramide synthesis using different fatty acyl-CoA donors. J Biol Chem 278:43452–43459

Schorling S, Vallée B, Barz WP, Riezman H, Oesterhelt D (2001) Lag1p and Lac1p are essential for the Acyl-CoA-dependent ceramide synthase reaction in *Saccharomyces cerevisae*. Mol Biol Cell 12:3417–3427

Sridevi P, Alexander H, Laviad EL, Pewzner-Jung Y, Hannink M, Futerman AH, Alexander S (2009) Ceramide synthase 1 is regulated by proteasomal mediated turnover. Biochim Biophys Acta 1793:1218–1227

Trapp BD, Kidd GJ, Hauer P, Mulrenin E, Haney CA, Andrews SB (1995) Polarization of myelinating Schwann cell surface membranes: role of microtubules and the trans-Golgi network. J Neurosci 15:1797–1807

Voelzmann A, Bauer R (2010) Ceramide synthases in mammalians, worms, and insects: emerging schemes. BioMol Concept 1:411–422

Yu J-Y, Chung K-H, Deo M, Thompson RC, Turner DL (2008) MicroRNA miR-124 regulates neurite outgrowth during neuronal differentiation. Exp Cell Res 314:2618–2633

Yu RK, Nakatani Y, Yanagisawa M (2009) The role of glycosphingolipid metabolism in the developing brain. J Lipid Res 50(Suppl):S440–S445